

## Image Color and Texture-based Modeling and Simulation of Ripeness Identification for Fresh Corn Ears

Huihui Wang<sup>1</sup>, Yan Lv<sup>1</sup>, Yonghai Sun<sup>2</sup>, Xuejun Wang<sup>1</sup>, Xueheng Tao<sup>1</sup>  
and Jixin Yang<sup>1</sup>

<sup>1</sup> School of Mechanical Engineering and Automation, Dalian Polytechnic University  
Dalian, China

<sup>2</sup> School of Biological and Agricultural Engineering, Jilin University  
Changchun, China

<sup>1</sup>whh419@126.com

### Abstract

*In this study, an identification model based on computer vision and artificial neural network technologies is proposed for the identification of the ripeness of fresh corn ears. For collected images of corn ears, 2D discrete wavelet transform is performed to extract information of low-frequency sub-band as color features, and discrete Fourier transform is performed to extract energy spectrum information as texture features. Principle component analysis is employed for the fusion and dimensionality reduction of color and texture features, and the first three principle components are chosen as inputs of the network model in order to establish probabilistic neural network model for the automated ripeness identification of fresh corn ears. Simulation analysis demonstrates that the identification accuracy of this model reaches 90.67%.*

**Keywords:** Fresh corn ear, Color, Texture, Identification model, Simulation

### 1. Introduction

Fresh corn ears contain various amino acids, vitamins, trace elements, fatty acids, and other nutritional components, endowing them with some medical and health effects. With the increasing recognition of corn ears' nutritional value, the demand for fresh corn ears in China is also gradually increasing [1-3]. Generally, corn ears as fresh food are in milk stage, when both the nutritional value and eating quality of the ears are much higher than those in other stages. On the other hand, ears with different ripeness should be processed with different ripening technologies. Therefore, the ripeness of fresh corn ear is an important indicator for its quality inspecting and processing [4]. Currently, ripeness identification of fresh corn ears mainly depends on manual work, which is highly intense and subjective [5]. In this paper, a ripeness identification model is presented to automate this process. This model is designed using computer vision technology; from images of fresh corn ears, color features are extracted in wavelet domain, and texture features are extracted based on Fourier transform. After optimizing the multiple features through principle component analysis, the model is established using artificial neural network technology. Simulation analysis is performed to validate the model.

## 2. Theory of Image-based Ripeness Identification for Fresh Corn Ears

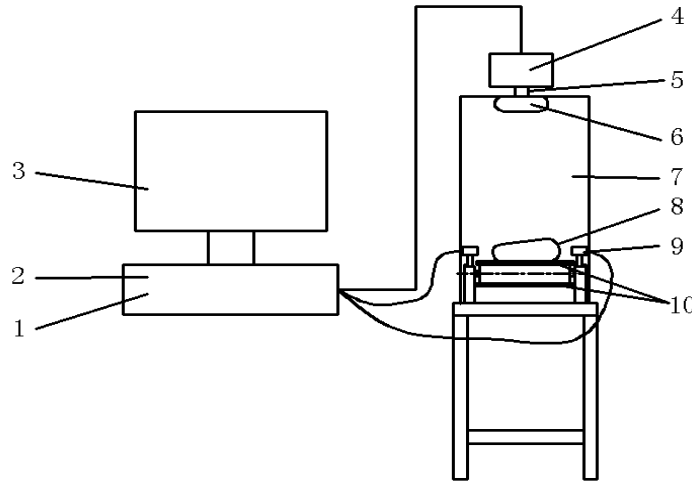


**Figure 1. Diagram of the image collection system**

1. Image acquisition card
2. Data acquisition card
3. Computer
4. Industrial camera
5. Camera lens
6. Ring-shaped light source
7. Test box
8. Corn ear
9. Photoelectric switch
10. Conveyor

Cleaned whole ears of corns of cultivar “Kennian No.1” with husk leaves removed are used in this experiment. Ears are classified into three grades according to ripeness, grade 1 ears are milk stage ears, which are the most edible; grade 2 ears are in post-milk stage, with poor eating quality; grade 3 ears are in pre-milk stage and cannot be eaten. Images of the corn ears are collected with the equipment shown in Figure 1. Ears are transported by the conveyor; when an ear passes the photoelectric switch, data acquisition card receives a triggering signal and dictates image acquisition card to collect an image of the ear. A sample image is as shown in Figure 2. Images of middle parts of corn ears are collected as 24-bits BMP in 480 x 360 pixels.



**Figure 2. A sample image of corn ear**

Since fresh corn ears with different ripeness exhibit different colors and textures, in this study color and texture features are primarily employed for the identification of ear ripeness. Both human eyes and computer are endowed with certain resolutions, and cannot identify signals lower than certain scales. Meanwhile, wavelet transform can decompose signals at different scales, and the approximations of the images in wavelet domain mainly concentrate in the low-frequency part. Therefore, the collected images are performed 2D discrete wavelet

transform in order to extract the low-frequency information as color features for ripeness identification. On the other hand, after Fourier transform, most interference signals in spatial domain can be removed, and the size and distribution of energy spectrum of the two-dimensional images are closely related to texture. Therefore, Fourier transform is employed for the analysis of image energy spectrum in order to extract energy spectrum information as texture features for ripeness identification. To avoid massive computation and reduce processing time, principle component analysis is performed to the extracted color and texture features for fusion and dimensionality reduction of the feature parameters. At last, probabilistic neural network (PNN), which has simple structure, few parameters and strong classification ability, is chosen to train the selected features for ripeness identification of fresh corn ears.

### 3. Image-based Ripeness Identification Model for Fresh Corn Ears

#### 3.1. Extraction of color features

HIS color model, which is more in line with human being's convention in describing colors, is chosen for the color feature-based wavelet transform feature extraction [6]. The collected images are first performed RGB to HSI model transform, and the H component, stands for hue, is performed 2D discrete wavelet transform.

##### 3.1.1. Identification of the number of wavelet decomposition levels

After wavelet transform, color information of corn ears are mainly distributed in low-frequency sub-band, while edge detail information is mainly distributed in high-frequency sub-bands.  $LL_j$ ,  $HL_j$ ,  $LH_j$  and  $HH_j$  are used to denote the low- and high-frequency sub-bands of the  $j$ -th level of ear images. If the decomposition of the  $j$ -th level is denoted by  $P_j$ , the ratio of energy sum of three high-frequency sub-bands  $HL_j$ ,  $LH_j$  and  $HH_j$  to the total energy is:

$$P_j = \frac{EN_{HL_j} + EN_{LH_j} + EN_{HH_j}}{EN} \quad (1)$$

$$E_{HL_j} = \sum_x \sum_y f_{HL_j}^2(x, y) \quad (2)$$

$$E_{LH_j} = \sum_x \sum_y f_{LH_j}^2(x, y) \quad (3)$$

$$EN_{HH_j} = \sum_x \sum_y f_{HH_j}^2(x, y) \quad (4)$$

Where,  $EN_{HL_j}$ ,  $EN_{LH_j}$  and  $EN_{HH_j}$  indicate energies of the three high-frequency sub-bands  $HL_j$ ,  $LH_j$  and  $HH_j$ , respectively.

$f_{HL_j}(x, y)$ ,  $f_{LH_j}(x, y)$  and  $f_{HH_j}(x, y)$  are wavelet coefficients of the three high-frequency sub-bands  $HL_j$ ,  $LH_j$  and  $HH_j$ , respectively.

$EN$  is the total energy of the corn ear image.

To study energy correlation of two adjacent levels, the ratio  $S_j$  of level  $P_j$  to its previous level is:

$$S_j = \frac{P_j}{P_{j-1}} \quad j = 2, \dots, j_{\max} \quad (5)$$

Where,  $j_{\max}$  is the optimum number of decomposition levels for the ripeness identification of fresh corn ears.

Since the images collected in this study are in 480x380 pixels, the approximate size of each sub-band after five levels of wavelet transform is about 1x1 pixels. In such case, any more transform is meaningless, therefore we define the range of  $j_{\max}$  as 1-5. For low-frequency sub-band, extraction of color features is primarily performed, therefore the optimal number of decomposition levels is the number when color information accounts for the highest proportion of the low-frequency sub-band, i.e. when edge information is mostly separated. At this time,  $S_j$  is the smallest, and the number of decomposition levels  $j$  equals to  $j_{\max}$  [7].

Images of totally 150 corn ears are collected and performed the transforms and calculation described above. Wavelet transform of 1 to 5 levels is performed to the value of the  $H$  component and the average value  $\bar{S}_j$  of  $S_j$  is calculated. As shown in Table 1,  $\bar{S}_j$  increases with the number of decomposition levels. Taking processing time and computational complexity into account, we identify the number of wavelet transform levels as 2.

**Table 1. Average value  $\bar{S}_j$  of  $S_j$  of fresh corn ear local images**

| Number of decomposition levels | $j=2$ | $j=3$ | $j=4$ | $j=5$ |
|--------------------------------|-------|-------|-------|-------|
| $\bar{S}_j$                    | 0.394 | 0.493 | 1.190 | 1.237 |

### 3.1.2. Extraction of color features

After 2 levels of wavelet transform to the ear images, color information and energy pertinent to ripeness mainly concentrate in the low-frequency sub-band. Therefore, we extract the wavelet coefficients of sub-band  $LL_2$  and calculate their average value  $A$ , variance  $V$ , average energy  $N_a$ , and color entropy  $N_t$  as the color features representing ear ripeness. The four features are calculated by:

$$A = \frac{1}{Le \times Wi} \sum_x \sum_y f_{LL_2}(x, y) \quad (6)$$

$$V = \frac{1}{Le \times Wi} \sum_x \sum_y [f_{LL_2}(x, y) - A]^2 \quad (7)$$

$$N_a = \frac{1}{Le \times Wi} \sum_x \sum_y f_{LL_2}^2(x, y) \quad (8)$$

$$N_t = \frac{1}{Le \times Wi} \sum_x \sum_y f_{LL_2}(x, y) \lg \sum_x \sum_y f_{LL_2}(x, y) \quad (9)$$

Where,  $Le \times Wi$  is the size of the low-frequency sub-band, and  $f_{LL_2}(x, y)$  is the wavelet coefficient corresponding to  $LL_2$ .

### 3.2. Extraction of texture features

To extract texture features, one-dimensional Fourier transform is firstly performed to ear images. For a one-dimensional function  $f(x)$  which has definite numbers of intervals and extreme points, and is absolutely integrable, its Fourier transform is:

$$F(\mu) = \int_{-\infty}^{+\infty} f(x)e^{-j2\pi\mu x} dx \quad (10)$$

Where,  $x$  is time domain variable and  $\mu$  is frequency domain variable.

Let  $\omega = 2\pi\mu$ , then

$$F(\omega) = \int_{-\infty}^{+\infty} f(x)e^{-j\omega x} dx \quad (11)$$

Indicate the real and imaginary parts of  $F(\mu)$  by  $R(\omega)$  and  $I(\omega)$ , then the expressions of complex functions of Fourier transform are:

$$F(\omega) = R(\omega) + I(\omega) \quad (12)$$

$$|F(\omega)| = \sqrt{R^2(\omega) + I^2(\omega)} \quad (13)$$

Extend the above transform to two dimensions and let the two-dimensional function be  $f(x, y)$ , then:

$$F(\mu, \nu) = \int_{-\infty}^{+\infty} \int_{-\infty}^{+\infty} f(x, y)e^{-j2\pi(\mu x + \nu y)} dx dy \quad (14)$$

$$|F(\mu, \nu)| = \sqrt{R^2(\mu, \nu) + I^2(\mu, \nu)} \quad (15)$$

Then the image energy spectrums can be expressed by:

$$E(\mu, \nu) = R^2(\mu, \nu) + I^2(\mu, \nu) \quad (16)$$

Assume the image size is  $M \times N$ , perform following discrete Fourier transform to fresh corn ear images:

$$F(\mu, \nu) = \sum_{x=0}^{M-1} \sum_{y=0}^{N-1} f(x, y)e^{-j2\pi(\frac{\mu x}{M} + \frac{\nu y}{N})} \quad (17)$$

With the center of an image as the origin, size and distribution of the energy spectrum along the circumferential direction is closely related to thickness of the image's texture. When texture is thick, energy concentrates near the origin, while energy spreads to peripheral area when texture is thin. Radial energy of the energy spectrum is closely related to texture direction, more energy concentrates on vertical

direction of the texture [8]. Since fresh corn ears of different ripeness exhibit different texture features, size and distribution of the energy spectrum are analyzed to study texture features, in order to extract the information pertinent to ripeness.

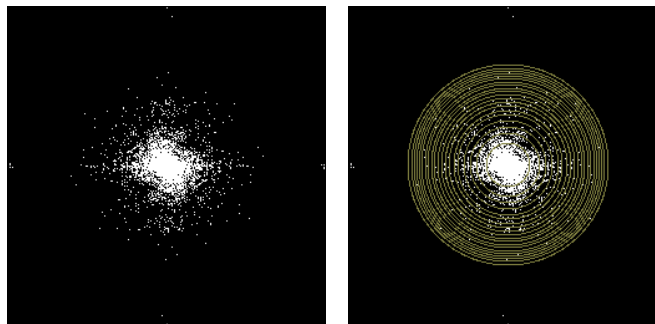
Energy spectrum of an image after 2D discrete Fourier transform is presented in Figure 3(a). It can be seen that the energy spectrum is in a ring-like shape. Therefore, we draw evenly spaced concentric circles around the image center, which is also the center of the spectrum, as shown in Figure 3(b). In this study, we call these circles energy circles. For each energy circle, the ratio of energy inside the circle to the total energy is obtained as the feature value for texture analysis. For an image of the size of  $L \times W$ , the energy spectrum of Fourier transform is:

$$P(u, v) = |F(u, v)|^2 \quad (18)$$

The ratios obtained are:

$$p_i = \frac{E_i}{\sum_{u=0}^L \sum_{v=0}^W P(u, v)} \quad i=1,2,\dots,20 \quad (19)$$

Where,  $E_i$  is the total energy inside the  $i$ -th circle.



(a) Energy spectrum      (b) Energy circles

**Figure 3. Energy spectrum of corn ears**

As mentioned, 150 corn ears are used in this experiment. Ripeness identification to 75 of these 150 ears is firstly performed by experienced inspectors. The numbers of grade 1, 2 and 3 ears are 20, 30 and 25, respectively. Discrete Fourier transform is then performed to images of these 75 corn ears in order to obtain energy spectrums and calculate the values of  $p_i$ . Table 2 presents the ranges that the  $p_i$  values of the first five circles of the images are in. Energy of the images of ears with different ripeness mostly concentrate in the circles near the center, thus  $p_1$  has the biggest value, and  $p_i$  value decreases along with the circles expand outward. For most grade 2 ears,  $p_i$  values are smaller than 0.1 and approaching 0, some are already 0, when  $i$  is equal to or smaller than 3. For grade 1 and 3 ears,  $p_i$  values are smaller than 0.1 and approaching 0 when  $i$  is equal to or smaller than 4 or 5. Therefore, for energy spectrum of images of corn ears with any ripeness, extracting  $p_i$  values when  $i$  is in the range of 1~5 as texture features is sufficient.

**Table 1. Ranges of  $p$  values of images of corn ears with different ripeness**

| Ripeness Grade | $i=1$       | $i=2$       | $i=3$       | $i=4$       | $i=5$       |
|----------------|-------------|-------------|-------------|-------------|-------------|
| 1              | [0.34,0.57] | [0.19,0.25] | [0.06,0.13] | [0.04,0.08] | [0.02,0.06] |
| 2              | [0.64,1.00] | [0.00,0.25] | [0.00,0.07] | [0.00,0.04] | [0.00,0.00] |
| 3              | [0.31,0.62] | [0.19,0.28] | [0.06,0.14] | [0.02,0.09] | [0.00,0.07] |

### 3.3. Optimization of feature parameters

Based on the discussion above, 2D discrete wavelet two-level decomposition is performed to images of the fresh corn ears. Four color feature parameters are extracted, including average value  $A$ , variance  $V$ , average energy  $N_a$  and color entropy  $N_l$  of the  $LL_2$  sub-band in HSI model. Discrete Fourier transform is performed to the images to obtain energy spectrums and calculate the values of  $p_1, p_2, p_3, p_4$  and  $p_5$ .

If these nine parameters are all used as feature parameters to perform ripeness identification, the computational complexity is high and the algorithm is complicated. Therefore, principle component analysis is performed for dimensionality reduction. With images of all 150 corn ears as samples, extract image parameters and obtain sample matrix  $W$  as below.

$$W = \begin{bmatrix} w_{11} & w_{21} & \cdots & w_{p1} \\ w_{12} & w_{22} & \cdots & w_{p2} \\ \vdots & \vdots & \vdots & \vdots \\ w_{1q} & w_{2q} & \cdots & w_{pq} \end{bmatrix} \quad (20)$$

Where,  $p$  is the number of samples and equals to 150,  $q$  is the number of color and texture features and equals to 9.

To eliminate the dimensional impacts between the feature parameters, standardize  $W$  and matrix  $W'$  as below is obtained.

$$W' = \begin{bmatrix} w'_{11} & w'_{21} & \cdots & w'_{p1} \\ w'_{12} & w'_{22} & \cdots & w'_{p2} \\ \vdots & \vdots & \vdots & \vdots \\ w'_{1q} & w'_{2q} & \cdots & w'_{pq} \end{bmatrix} \quad (21)$$

Based on correlation coefficient matrix  $R_w$ , compute feature value  $\lambda_i (i=1, \dots, n)$ , corresponding matrix  $U$  of unit feature vectors, and contribution rates, matrix  $U$  as shown in Expression (22) is obtained.

$$U = \begin{bmatrix} u_{11} & u_{21} & \cdots & u_{n1} \\ u_{12} & u_{22} & \cdots & u_{n2} \\ \vdots & \vdots & \vdots & \vdots \\ u_{1n} & u_{2n} & \cdots & u_{nn} \end{bmatrix} = (U_1, U_2, \dots, U_n) \quad (22)$$

Where,  $n = 9$ .

With the discussion above, calculate the principle components. Denote principle components with  $F$ , and feature values and contribution rates of the nine principle components are as presented in Table 3.

$$F = U^T W' \quad (23)$$

**Table 3. Feature values and contribution rates of principle components**

| Principle components | Feature value $\lambda$ | Contribution rate (%) | Accumulated contribution rate (%) |
|----------------------|-------------------------|-----------------------|-----------------------------------|
| 1                    | 4.465                   | 49.607                | 49.607                            |
| 2                    | 2.482                   | 27.577                | 77.183                            |
| 3                    | 1.165                   | 12.948                | 90.131                            |
| 4                    | 0.465                   | 5.171                 | 95.302                            |
| 5                    | 0.313                   | 3.480                 | 98.782                            |
| 6                    | 0.088                   | 0.973                 | 99.755                            |
| 7                    | 0.015                   | 0.170                 | 99.925                            |
| 8                    | 0.007                   | 0.074                 | 99.999                            |
| 9                    | 0.000                   | 0.001                 | 100.000                           |

According to the accumulated contribution rates in Table 3, the first three principle components already have an accumulated contribution rate of 90.131%, exceeds 85%. Therefore, the first three principle components are sufficient enough to extract 90.131% of the information represented by all nine principle components, and the represented information is not overlapped.

### 3.3. Establishment of the ripeness identification model

Probabilistic neural network (PNN) is a parallel algorithm carried out on the basis of Minimum Bayes-Risk rules. Since in PNN, kernel functions with any estimated probability density can be chosen as transfer function of pattern layer, it is suitable for both online production and real-time processing[9,10]. In this study, PNN is chosen for the ripeness identification of fresh corn ears.

In this study, PNN is constructed in following procedure:

- a. Set the number of neurons in input layer as 3; the three units are the 1<sup>st</sup>, 2<sup>nd</sup> and 3<sup>rd</sup> principle components from the principle component analysis, respectively.
- b. Hidden neurons are determined by the network in a self-adaptive manner.
- c. With experiments on extended constants of the 150 corn ears, the network classification is the fastest and with best effects when the extended constant is 0.1.



- d. Set the number of neurons in output layer as 3, indicating the three grades of ear ripeness.
- e. From the 150 corn ears, choose the 75 ears with known ripeness and use their images as network training samples, and complete the construction of the ripeness identification model.

#### 4. Simulation Analysis

To validate the ripeness identification model established in this study, ripeness identification is performed to 75 ears out of the 150 samples besides the training samples by experienced inspectors first. The numbers of grade 1, 2 and 3 ears are 23, 30, and 22, respectively. Images of these ears are input into the established ripeness identification model as test samples, and the identification result is as shown in Table 4.

**Table 4. Feature values and contribution rates of principle components**

| Manual Classification | Number of Test Samples | PNN classification result |    |    | Identification Accuracy (%) |
|-----------------------|------------------------|---------------------------|----|----|-----------------------------|
|                       |                        | 1                         | 2  | 3  |                             |
| 1                     | 23                     | 20                        | 0  | 3  | 90.67                       |
| 2                     | 30                     | 1                         | 29 | 0  |                             |
| 3                     | 22                     | 3                         | 0  | 19 |                             |

The model has an identification accuracy of 90.67%, with only one of the 30 grade 2 ear samples is misidentified. For grade 1 and 3 ears, misidentification rate is relatively high, mainly because grade 1 and 3 ears have very similar color features, while both the color and texture features of grade 2 ears exhibit obvious difference with ears of the other two ripeness grades.

#### 5. Conclusions

Aiming at the recent high demand for fresh corn ears, and the fact that ripeness identification highly depends on manual work, a modeling method using computer vision and neural network technologies. Color and texture features of images of fresh corn ears are extracted with image processing technology. Dimensionality reduction is then performed to the extracted features through principle component analysis. Based on probabilistic neural network, a ripeness identification model is established. Simulation with the model shows that it can fulfill the primary accuracy requirement of ripeness identification in actual production. With more effective color feature extraction, we expect to improve the identification accuracy of grade 1 and 3 corn ears.

#### Acknowledgements

This study is supported by the National Science and Technology Doctoral Initiation Project of Liaoning Province (No. 20121098) and General Projects of Science and Technology Study of Liaoning Department of Education (No. L2012193).

## References

- [1] S. Hooda and A. Kawatra, "Effect of frozen storage on nutritional composition of baby corn", *Nutrition & Food Science*, vol. 42, no. 1, (2012), pp. 5-11.
- [2] C. M. Bandei, W. P. Evangelist and M. B. A. Gloria, "Bioactive amines in fresh canned and dried sweet corn embryo and endosperm and germinated corn", *Food Chemistry*, vol. 131, no. 4, (2012), pp. 1355-1359.
- [3] S. Hooda and A. Kawatra, "Nutritional evaluation of baby corn (zea mays)", *Nutrition & Food Science*, vol. 43, no. 1, (2013), pp. 68-73.
- [4] P. Zhang, J. Si, L. Wang and Z. Ren, "Effect of Different Harvest Maturities on the Carbohydrate Content of Corn with Different Variations during the Storage", *Storage & Process*, no. 5, (2012), pp. 14-17.
- [5] H. Li, S. Dong and R. Gao, "Research on Quality Characteristic of Fresh Corn", *Journal of Maize Sciences*, no. 2, (2007), pp. 144-147.
- [6] K. Deb, I. Khan, A. Saha and K.-H. Jo, "An Efficient Method of Vehicle License Plate Recognition Based on Sliding Concentric Windows and Artificial Neural Network", *Procedia Technology*, vol. 4, (2012), pp. 812-819.
- [7] H. Wang, Y. Sun, J. Liu, T. Zhang, X. Wang and Y. Li, "Evaluation of Maturity Grading for Fresh Corn Ear Based on Two-dimension Discrete Wavelet", *Jurnal of Jilin University Engineering and Technology Edion*, vol. 41, no. 2, (2011), pp. 574-578.
- [8] Z. Yunlong, F. Zhenru, S. Yaolei and Y. Li, "Identification method of flow regime based on images texture features by fourier transform and probabilistic neural network in gas-solid fluidized bed's", *Control and Instruments in Chemical Industry*, vol. 36, no. 2, (2009), pp. 38-42.
- [9] F. H. Fan, Q. Ma, J. Ge, Q. Y. Peng, W. W. Riley and S. Z. Tang, "Prediction of texture characteristics from extrusion food surface images using a computer vision system and artificial neural networks", *Journal of Food Engineering*, vol. 118, no. 4, (2013), pp. 426-433.
- [10] G. A. Leiva-Valenzuela and J. M. Aguilera, "Automatic detection of orientation and diseases in blueberries using image analysis to improve their postharvest storage quality", *Food Control*, vol. 33, no. 1, (2013), pp. 166-173.